Published OnlineFirst January 13, 2014; DOI: 10.1158/1535-7163.MCT-13-0395

The Selective Anaplastic Lymphoma Receptor Tyrosine Kinase Inhibitor ASP3026 Induces Tumor Regression and Prolongs Survival in Non–Small Cell Lung Cancer Model Mice

Masamichi Mori, Yoko Ueno, Satoshi Konagai, Hiroshi Fushiki, Itsuro Shimada, Yutaka Kondoh, Rika Saito, Kenichi Mori, Nobuaki Shindou, Takatoshi Soga, Hideki Sakagami, Takashi Furutani, Hitoshi Doihara, Masafumi Kudoh, and Sadao Kuromitsu

Abstract

Activation of anaplastic lymphoma receptor tyrosine kinase (ALK) is involved in the pathogenesis of several carcinomas, including non–small cell lung cancer (NSCLC). Echinoderm microtubule–associated protein like 4 (EML4)-ALK, which is derived from the rearrangement of *ALK* and *EML4* genes, has been validated as a therapeutic target in a subset of patients with NSCLC. Here, we investigated the effects of ASP3026, a novel small-molecule ALK inhibitor, against ALK-driven NSCLC. ASP3026 inhibited ALK activity in an ATP-competitive manner and had an inhibitory spectrum that differed from that of crizotinib, a dual ALK/MET inhibitor. In mice xenografted with NCI-H2228 cells expressing EML4-ALK, orally administered ASP3026 was well absorbed in tumor tissues, reaching concentrations >10-fold higher than those in plasma, and induced tumor regression with a wide therapeutic margin between efficacious and toxic doses. In the same mouse model, ASP3026 enhanced the antitumor activities of paclitaxel and pemetrexed without affecting body weight. ASP3026 also showed potent antitumor activities, including tumor shrinkage to a nondetectable level, in *hEML4-ALK* transgenic mice and prolonged survival in mice with intrapleural NCI-H2228 xenografts. In an intrahepatic xenograft model using NCI-H2228 cells, ASP3026 induced continuous tumor regression, whereas mice treated with crizotinib showed tumor relapse after an initial response. Finally, ASP3026 exhibited potent antitumor activity against cells expressing EML4-ALK with a mutation in the gatekeeper position (L1196M) that confers crizotinib resistance. Taken together, these findings indicate that ASP3026 has potential efficacy for NSCLC and is expected to improve the therapeutic outcomes of patients with cancer with ALK abnormality. *Mol Cancer Ther; 13(2); 329–40. ©2014 AACR.*

Introduction

Lung cancer is the most commonly diagnosed cancer and the leading cause of cancer-related deaths worldwide (1). Treatment outcomes with conventional antitumor drugs in advanced or metastatic non–small cell lung cancer (NSCLC) remain unsatisfactory due to low rates of response and long-term survival (2). However, in the last few decades, investigations of the molecular mechanisms of cancer pathogenesis have identified several cancer drivers, such as receptor tyrosine kinases (TK), which have been used for new, targeted therapies against several types of cancers, including NSCLC (3–8). Such therapies have markedly improved response rates and survival outcomes of patients with cancer, and represent a paradigm shift in cancer treatment. For example, the driver tyrosine kinase BCR-ABL is implicated in the pathogenesis of chronic myeloid leukemia, and imatinib, an inhibitor of BCR-ABL, induces hematologic and cytogenetic responses that help prevent disease progression (3, 4). Targeted therapies against cancer drivers have also proved effective against solid malignancies, such as the use of trastuzumab against HER2 in breast cancer (5), gefitinib and erlotinib against EGF receptor (EGFR) in NSCLC (6–8), and vemurafenib against BRAF V600E in melanoma (9).

EML4-ALK is a fusion gene comprising portions of the echinoderm microtubule–associated protein like 4 (*EML4*) and anaplastic lymphoma kinase (*ALK*) genes, and was first found in a subset of NSCLC cells (10, 11). Soda and colleagues (10) discovered *EML4-ALK* by screening a retroviral complementary DNA expression library generated from a lung adenocarcinoma specimen surgically resected from a 62-year-old man with a smoking history. *EML4-ALK* was formed through disruption

Authors' Affiliation: Drug Discovery Research, Astellas Pharma Inc., Tsukuba-shi, Ibaraki, Japan

Note: Supplementary data for this article are available at Molecular Cancer Therapeutics Online (http://mct.aacrjournals.org/).

Corresponding Author: Masamichi Mori, Pharmacology Research Labs, Oncology, Drug Discovery Research, Astellas Pharma Inc., 21, Miyukigaoka, Tsukuba-shi, Ibaraki 305-8585, Japan. Phone: 81-298-636-584; Fax: 81-298-522-955; E-mail: masamichi.mori@astellas.com

doi: 10.1158/1535-7163.MCT-13-0395

Published OnlineFirst January 13, 2014; DOI: 10.1158/1535-7163.MCT-13-0395

of *EML4* at a position approximately 3.6-kb downstream of exon 13 and ligation to a position 297-bp upstream of exon 21 of *ALK*. EML4-ALK has transforming potential that is dependent on its kinase activity, while the coiled-coil domain of EML4 mediates the constitutive dimerization and cytoplasmic activation of EML4-ALK, which together are responsible for the generation of transformed cell foci *in vitro* and tumor formation in nude mice (10). Separately, Rikova and colleagues (11) discovered a variant of EML4-ALK, in which intron 6 of *EML4* is fused to the *ALK* gene, and another ALK fusion protein, TRK-fused gene (TFG)-ALK, during phosphoproteomic analyses of tyrosine signaling. More recently, Takeuchi and colleagues (12) identified a novel oncokinase fusion protein, kinesin family member 5B (KIF5B)-ALK, using an immunohistochemistry-based diagnostic system. The identification of these various ALK fusion proteins indicates that the kinase activity of ALK plays an important role in the pathogenesis of a subset of NSCLC. In addition, treatment of spontaneous pulmonary tumor in *hEML4-ALK* transgenic mice with an ALK inhibitor or repression of ALK expression results in tumor regression (13, 14). Together, these experimental evidences suggest that EML4-ALK is a targetable genetic lesion in NSCLC (15).

ALKoma, tumors carrying abnormal ALK as an essential growth driver, has also been found in several cancer types other than NSCLC (16). In these tumor cells, ALK is rendered oncogenic as a result of its fusion to various proteins, including nucleophosmin (nucleolar phosphoprotein B23, numatrin) in anaplastic large cell lymphoma (17), tropomyosin 3 or 4 in inflammatory myofibroblastic tumors (18), vinculin in renal medullary carcinoma (19, 20), and clathrin in ALK-positive diffuse large B-cell lymphoma (21). In addition, activated mutation of ALK is also involved in the development of neuroblastoma and anaplastic thyroid cancer (22, 23). Several ALK inhibitors with efficacy against ALKoma in preclinical models and patients have been identified (24–27). For example, the small-molecule ALK and MET inhibitor crizotinib exhibited high efficacy with overall response rates of $\geq$50% in clinical trials of patients with NSCLC harboring an EML4-ALK oncogenic kinase (28, 29). However, the treatment was not curative, and the patients developed resistance in target lesions and/or metastatic sites and had a progression-free survival of only approximately 10 months (28–30). Two secondary point mutations (L1196M and C1156Y) have been identified within the kinase domain of EML4-ALK in tumor cells isolated from a patient who relapsed after an initial response to crizotinib (31). The point mutation L1196M is analogous to other kinase domain mutations, including the T790M mutation in EGFR (32) and T315I mutation in BCR-ABL (33), in gatekeeper positions seen in patients who developed resistance to tyrosine kinase inhibitor (TKI) treatment (33). The gatekeeper position including the L1196M mutation site is located at the bottom of the ATP-binding pocket of EML4-ALK, and the presence of an amino acid with a bulky side chain at this position interferes with the interaction of the TKI with the kinase domain of the target protein, thereby decreasing the efficacy of treatment (34). Thus, more potent ALK inhibitors, such as those capable of inhibiting L1196M ALK, are needed to overcome the resistance that often develops in both lung and metastatic sites.

In the present study, we characterized a recently discovered novel and selective small-molecule ALK inhibitor, ASP3026, against ALK-driven NSCLC tumors in a nonclinical setting. We examined the inhibitory effects of ASP3026 against ALK in cell-free systems and cellular assays, and evaluated the antitumor activity and survival benefits of ASP3026 in the mouse models with ALK-driven tumors in lung and metastatic sites. In addition, we also evaluated the antitumor activity of ASP3026 against cells expressing EML4-ALK with a mutation in the gatekeeper position and in combination with conventional antitumor agents in the mouse models of NSCLC.

Materials and Methods

Compounds, cell lines, and antibodies

ASP3026 (35) and crizotinib were synthesized by Astellas Pharma Inc. Paclitaxel and pemetrexed were purchased from LC Laboratories, and carboplatin was obtained from Bristol-Myers Squibb. NCI-H2228 cells were purchased from the American Type Culture Collection (ATCC) in July 2007 and authenticated by short tandem repeat profiling (Cell ID; Promega). H2228-luc cells, which exogenously express firefly luciferase, were prepared at Astellas Pharma Inc. 3T3 cells were obtained from ATCC in June 2007 (not authenticated) and were engineered to express either wild-type (EML4-ALK/3T3) or L1196M-mutated EML4-ALK (L1196M/3T3). Antibodies to ALK (C26G7), phosphorylated ALK (Tyr1604), p44/42 MAPK (Erk1/2), Phospho-p44/42 MAPK (Erk1/2; Thr202/Tyr204; 197G2), Phospho-Stat3 (Tyr705), Akt, and Phospho-Akt (Ser473; 193H12) were purchased from Cell Signaling Technology, Inc. Anti-actin antibody A2066 was purchased from Sigma-Aldrich Corporation.

Kinase inhibitory assays

EML4-ALK variant 1 kinase and its L1196M-mutated form were isolated from Ba/F3 cells transformed with the respective forms of EML4-ALK. Kinase activity was measured with HTRF KinEASE TK (SCETI Medical Labo K.K.) in the presence of various concentrations of ASP3026 or crizotinib.

An inhibitory assay for a panel of 86 tyrosine kinases (Supplementary Table S1) was conducted using ATP concentrations that were approximately equal to the K_m value for each kinase using a TK-ELISA or off-chip mobility shift assay at Carna Biosciences, Inc. The inhibitory percentage of ASP3026 and crizotinib against kinase activity was first determined at concentrations of 100 and 1,000 nmol/L in a single experiment. IC_{50} values were then separately determined in the presence of

Published OnlineFirst January 13, 2014; DOI: 10.1158/1535-7163.MCT-13-0395

various concentrations of each compound in three individual experiments.

Antiproliferative assays

NCI-H2228 cells were plated in RPMI-1640 supplemented with 10% heat-inactivated FBS in 96-well Sumilon celltight spheroid plates (Sumitomo Bakelite Co., Ltd.) at 2,000 cells per well and then incubated at 37°C in a 5% CO_2 atmosphere overnight. The cells were exposed to test compounds, which were dissolved in dimethyl sulfoxide (DMSO) as a solvent, for 5 days, and viable cell numbers were then determined using the CellTiter-Glo Luminescent Cell Viability Assay (Promega). The IC_{50} value of each compound was calculated by nonlinear regression analysis using the Sigmoid–Emax model, and the mean IC_{50} values were calculated from four individual experiments. In the assay with 3T3 cells, the cells were plated in Dulbecco's Modified Eagle Medium (DMEM) supplemented with 10% heat-inactivated FBS in 96-well spheroid plates (Sumitomo Bakelite Co., Ltd.) at 500 cells per well, incubated overnight, and then treated with the test compounds for 2 days. The IC_{50} values were determined from a single experiment.

Immunoblotting

NCI-H2228 cells were seeded at 4 to 5 $\times$ 10^5 cells per well in 12-well HydroCell plates (CellSeed), incubated for 2 days, and ASP3026 was then added to each well at a final concentration of 0 (DMSO), 10, 100, or 1,000 nmol/L. Cell lysates were prepared for immunoblot analysis of EML4-ALK, ERK, STAT3, AKT, and actin after 4 hours of ASP3026 treatment. In an *in vivo* experiment, mice with NCI-H2228 tumors were treated with ASP3026 at a single oral dose of 10 mg/kg, and tumors were then excised 4 hours after administration.

The lysates from cell and tumor samples were separated by electrophoresis and then transferred onto nitrocellulose membranes. After blocking with Blocking One or Blocking One-P (Nacalai Tesque) for 1 hour, each membrane was incubated with anti-ALK, anti-phospho-ALK, anti-ERK, anti-phospho-ERK, anti-phospho-STAT3, anti-AKT, or anti-phospho-AKT antibodies overnight at 4°C. The membranes were washed with 1× TBS Tween-20 Buffer (Thermo Fisher Scientific Inc.) and then incubated with anti-rabbit IgG (immunoglobulin G) HRP-linked antibody (Cell Signaling Technology) for 1 hour at room temperature. After a final washing, ECL Western Blotting Detection Reagents (GE Healthcare) were applied to the membranes, and signals were detected with a CCD camera (AISIN) and quantified using a LumiVision PRO 400EX system (Taitec) or ImageJ software (NIH). The mean percentage of phosphorylated protein/total protein relative to that in vehicle-treated cells was then calculated.

In vivo models

All animal experimental procedures were approved by the Institutional Animal Care and Use Committee of Astellas Pharma Inc. Furthermore, Astellas Pharma Inc., Tsukuba Research Center was awarded accreditation status by AAALAC International. ASP3026 and crizotinib in a 0.5% methylcellulose solution were administered orally at once or twice daily doses starting after confirming tumor growth in each experiment. NCI-H2228 cells were subcutaneously inoculated into the flank of male nonobese diabetic/severe combined immunodeficient (NOD/SCID) mice (NOD.CB17-Prkdcscid/J; Charles River Laboratories Japan, Inc.) at 5 $\times$ 10^6 cells/0.1 mL per mouse. EML4-ALK/3T3 and EML4-ALK L196M/3T3 cells were subcutaneously inoculated into the flank of the male nude mice (CAnN.Cg-Foxn1nu/CrlCrlj[nu/nu]; Charles River Laboratories Japan, Inc.) at 3 $\times$ 10^6 cells/0.1 mL per mouse. Tumor diameter was measured using a caliper and tumor volume was determined by calculating the volume of an ellipsoid using the formula: length $\times$ width^2 $\times$ 0.5.

In an intrapleural xenograft model, H2228-luc cells were directly inoculated at 1 $\times$ 10^5 cells/20 μL per mouse into the pleural cavity of male NOD/SCID mice under anesthesia with isoflurane. In an intrahepatic xenograft model, H2228-luc cells were directly inoculated into the portal vein of male NOD/SCID mice at 1 $\times$ 10^6 cells/100 μL per mouse. Tumor growth was monitored by bioluminescent imaging (BLI) of the chest and abdominal areas with an IVIS Spectrum Imaging System (Caliper Life Sciences). The survival of mice was monitored daily.

hEML4-ALK transgenic mice were provided by Jichi Medical University (Tochigi, Japan) and were generated as previously described (13). Briefly, a complementary DNA fragment encoding EML4-ALK variant 1 was ligated to the surfactant protein C promoter and then injected into pronuclear-stage embryos of C57BL/6J mice. The tumors were monitored by computed tomography (CT) scan, which was performed for approximately 5 minutes under anesthesia induced with 2.5% isoflurane using an Inveon CT (Siemens). Data reconstruction and analysis were performed using Inveon Acquisition Workplace software (Siemens). Volumes of interests were manually drawn for pulmonary tumors detected in the CT images.

Pharmacokinetics

NOD/SCID mice subcutaneously xenografted with NCI-H2228 cells received a 5-day repeated oral dosing of 1, 3, and 10 mg/kg ASP3026 suspended in a 0.5% methylcellulose solution. Blood samples were collected from the inferior vena cava using a heparinized syringe, and plasma samples were prepared by centrifugation. Tumor samples were also collected from each mouse, and tumor weight was measured. The plasma and tumor concentrations of ASP3026 were measured using high-performance liquid chromatography-tandem mass spectrometry at Toray Research Center, Inc. C_{max}, T_{max}, and AUC_{0-24h} were calculated from the mean concentrations of ASP3026 using WinNonlin Professional V6.1 (Pharsight).

Published OnlineFirst January 13, 2014; DOI: 10.1158/1535-7163.MCT-13-0395

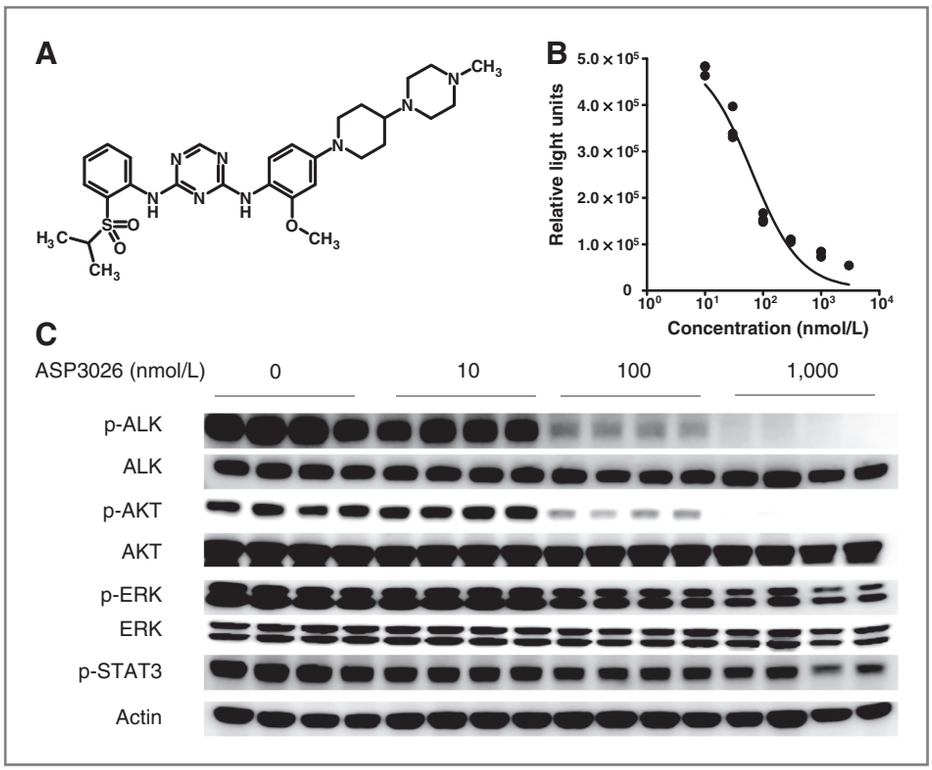

Figure 1. Structure and *in vitro* ALK inhibitory activity of ASP3026. A, chemical structure of ASP3026. B, antiproliferative activity of ASP3026 against NCI-H2228 NSCLC cells expressing EML4-ALK. The cells were seeded on spheroid plates and treated with various concentrations of ASP3026 for 5 days. Viable cell number was determined by the CellTiter-Glo Luminescent Cell Viability Assay to assess growth inhibition and is expressed as relative light units. Each point represents the mean relative luciferase units of triplicate replicates. The data are representative of four independent experiments. C, inhibition of ALK phosphorylation and signal transduction in NCI-H2228 cells by ASP3026. NCI-H2228 cells were treated with ASP3026 at the indicated concentrations for 4 hours, and each protein was detected by immunoblotting using specific antibodies.

Computational modeling

As the X-ray structures of both wild-type ALK and the L1196M variant of ALK with crizotinib (PDB IDs, 2XP2 and 2YFX) are publicly available, computation models of crizotinib were generated by adding missing hydrogen atoms and minimizing the coordinates of hydrogen atoms using Molecular Operating Environment (MOE, Chemical Computing Group Inc.). Docking simulation of ASP3026 with wild-type ALK was performed using the docking software Glide (Schrodinger, LLC). Wild-type ALK with NVP-TAE684 (PDB ID, 2XB7) was used as a template for the docking, and hydrogen atoms were added using MOE. The docking mode with the highest docking score was used in the modeling. The binding model of ASP3026 and ALK L1196M was generated by superimposing the backbone atoms of the protein coordinates over those of the 2YFX structure. All of the figures showing X-ray structures and docking results were constructed using MOE.

Results

ASP3026 inhibits the growth of ALK-dependent cells

ASP3026 was identified through a medicinal chemistry campaign (Fig. 1A) designed to obtain compounds with different profiles from a reported ALK inhibitor (35, 36). The kinase selectivity of ASP3026 was evaluated and compared with that of crizotinib against a panel of 86 tyrosine kinases (Supplementary Table S1). ASP3026 inhibited 11 tyrosine kinases by more than 50% at 1,000 nmol/L, and had the highest selectivity for ALK, ROS, and ACK kinases (Table 1). The kinase selectivity of ASP3026 clearly differed from that of crizotinib. Specifically, ASP3026 was more selective for FRK, YES, ACK, TNK1, and EGFR (L858R) among all tested kinases, whereas crizotinib had higher selectivity for MET, RON, LCK, JAK2, MUSK, TRKs, TYRO3, AXL, MER, and EPHs.

We next evaluated the antiproliferative activity of ASP3026 against NCI-H2228 NSCLC cells endogenously expressing EML4-ALK variant 3 using a spheroid cell culture system. After 5 days of treatment, ASP3026 inhibited the growth of NCI-H2228 cells with an IC_{50} value of 64.8 nmol/L (Fig. 1B). This value was higher than the concentration of ASP3026 required to achieve comparable results in the kinase inhibitory assays, and may possibly have been due to a higher ATP concentration in the NCI-H2228 NSCLC cells than that used in the assay. The growth suppression was accompanied by inhibition of ALK phosphorylation in the cells, in which the levels of phosphorylated ALK were 70%, 40%, and 9% after a 4-hour treatment with 10, 100, and 1,000 nmol/L ASP3026, respectively, compared with the vehicle-treated control cells (Fig. 1C). In addition, ASP3026 treatment also resulted in suppression of phosphorylation of AKT, ERK, and STAT3 at 100 and 1,000 nmol/L (Fig. 1C and Supplementary Table S2).

ASP3026 induces shrinkage of ALK-dependent NSCLC tumors

We next evaluated the antitumor activity of ASP3026 in a NCI-H2228 subcutaneous xenograft mouse model by

Published OnlineFirst January 13, 2014; DOI: 10.1158/1535-7163.MCT-13-0395

Table 1. Inhibitory activity of ASP3026 against various tyrosine kinases

	IC_{50} (nmol/L)	
TK	**ASP3026**	**Crizotinib**
wt ALK	3.5	1.5
F1174L ALK	10	1.8
R1275QALK	5.4	2
NPM1-ALK	6.8	2
ACK	5.8	>100
AXL	>100	3.3
L858R EGFR	86	>1,000
EPHA2	>1,000	54
EPHA6	>1,000	54
EPHB4	>1,000	68
FRK	40	1,000
JAK2	>1,000	11
LCK	>100	11
LTK	61	1.8
MER	>1,000	3.4
MET	>1,000	1.5
MUSK	>100	9.1
RON	>1,000	5.5
ROS	8.9	0.95
TNK1	26.8	>100
TRKA	>1,000	3.2
TRKB	>1,000	4.6
TRKC	>1,000	4.4
TYRO3	>1,000	20
YES	31.5	>100

NOTE: Inhibitory assay for the indicated tyrosine kinases (TK) was conducted using a TK-ELISA or Off-chip mobility shift assay. IC_{50} values were determined for tyrosine kinases that were inhibited by more than 50% at 100 nmol/L in three individual experiments.

examining the inhibitory effect of ASP3026 on ALK phosphorylation. A significant (approximately 20%; $P < 0.001$) decrease in phosphorylated ALK was observed 4 hours after a single oral administration of 10 mg/kg ASP3026 (Fig. 2A). In this model, once-daily oral administration of ASP3026 at 1, 3, 10, and 30 mg/kg/d for 2 weeks dose-dependently inhibited the growth of NCI-H2228 tumors by 69%, >100%, >100%, and >100%, respectively, and induced tumor regression by 0%, 4%, 45%, and 78%, respectively (Fig. 2B). Body weight was not affected by treatment with ASP3026 at any dose, even at 100 mg/kg twice daily (data not shown, Supplementary Fig. S1).

Consistent with the observed antitumor activity, ASP3026 was well absorbed after oral administration, with higher concentrations detected in tumor tissues than in plasma at each time point. The tumor/plasma ratios were 13 to 19 for Cmax and 19 to 23 for AUC_{0-24h} (Fig. 2C and Supplementary Table S3).

To further evaluate the antitumor activity of ASP3026, *hEML4-ALK* transgenic mice were treated with once-daily oral dosing of ASP3026 for 10 days after tumors were established in lungs. A series of CT scans taken during the treatment period clearly revealed a reduction of the tumor mass, with complete responses detected in 2 of 3 mice on day 7, and 3 of 3 mice on day 11 after the initiation of treatment at 100 mg/kg (Supplementary Fig. S2). A significant reduction of pulmonary tumor size in mice treated with 30 and 100 mg/kg ASP3026 was observed, as determined by the quantitative analysis of CT images taken on days 7 and 11 (Fig. 2D). The penetration of ASP3026 into tumors of this transgenic mouse model was confirmed by measurement of the drug concentration in tumors, which was more than 100-fold higher compared with those in plasma approximately 24 hours after the final dosing (data not shown).

ASP3026 enhances antitumor activities of paclitaxel and pemetrexed in mice with ALK-dependent NSCLC tumors

The antitumor activity of ASP3026 in combination with several NSCLC drugs was investigated in a subcutaneous NCI-H2228 xenograft model. Paclitaxel at 12 mg/kg induced tumor regression against NCI-H2228 xenografts, and the combination of paclitaxel with ASP3026 at 10 mg/kg caused further significant regression of tumors compared with each single-treatment group (Fig. 3A). Body weight loss was observed in the paclitaxel treatment groups, but by day 21, body weight had returned to the level at the initiation of treatment and did not significantly differ from the control mice. The difference of body weight between the combination and paclitaxel single-treatment groups did not largely change during the experiment. The combination of ASP3026 at 10 mg/kg with pemetrexed at 50 mg/kg was also effective at reducing tumor volume, which was smaller in the combination group than that in each single-treatment group (Fig. 3B). Pemetrexed treatment also induced body weight loss, which was not further induced by ASP3026. In contrast with paclitaxel and pemetrexed, ASP3026 did not enhance the antitumor activity of carboplatin (CBDCA) at 60 mg/kg in this model, as the tumor volume of the combination group was similar to that of the ASP3026 single-treatment group throughout the experimental period (Fig. 3C).

ASP3026 prolongs survival in mice with intrapleural xenografts of ALK-dependent NSCLC cells

We conducted antitumor assays for xenograft tumors in the pleural cavity, which is one of the major metastatic sites for NSCLC. H2228-luc cells were directly inoculated into the pleural cavity of mice, and the implanted cells were monitored using BLI of the chest area. The bioluminescent emissions of inoculated mice showed an approximately 100-fold increase during the 40-day period after cell inoculation and disease-related mortality was observed (Fig. 4A and Supplementary

Published OnlineFirst January 13, 2014; DOI: 10.1158/1535-7163.MCT-13-0395

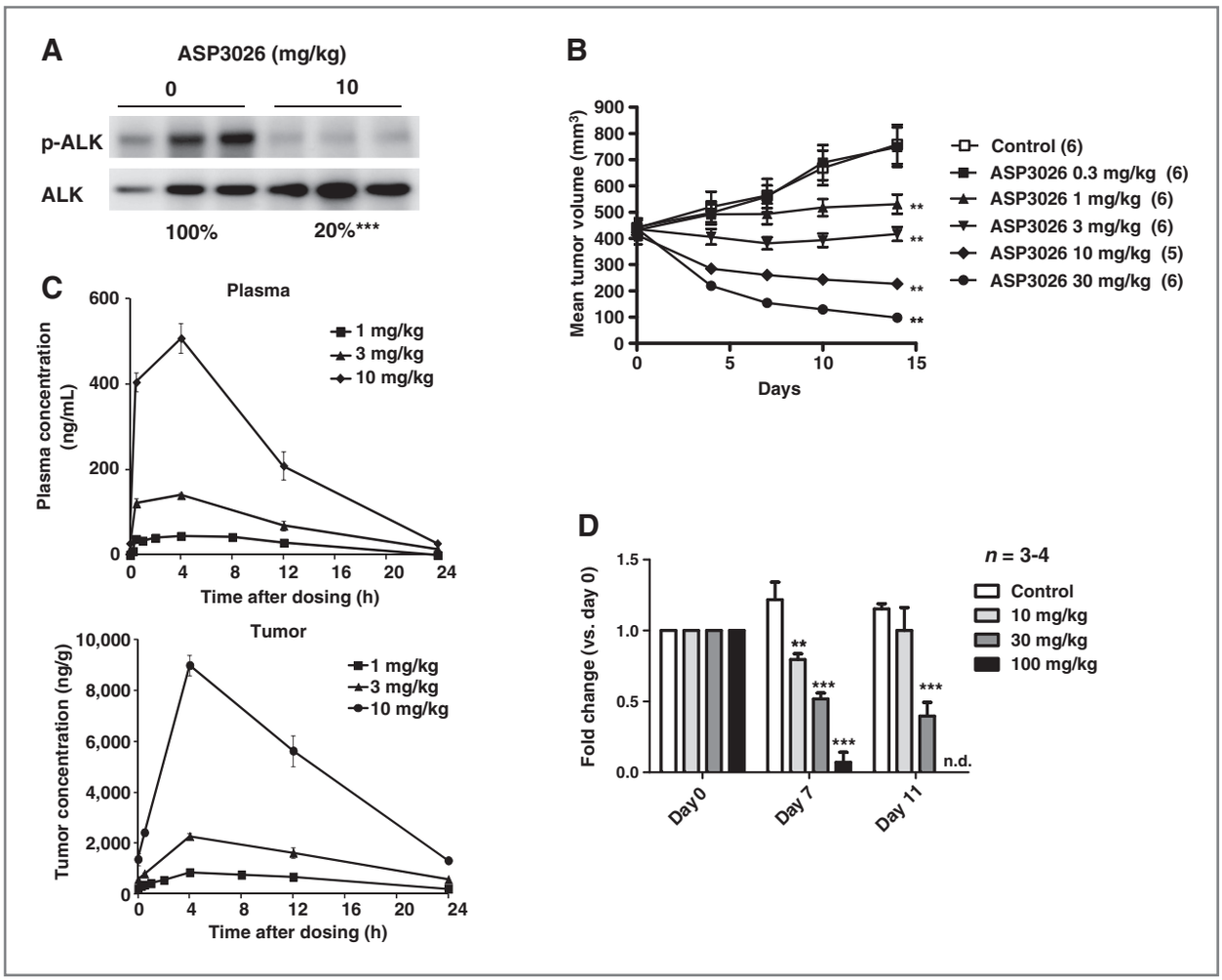

Figure 2. Antitumor activities of ASP3026 in a NCI-H2228 xenograft model and *hEML4-ALK* transgenic mice. A, inhibition of ALK phosphorylation in NCI-H2228 tumors by ASP3026. Mice with NCI-H2228 tumors were treated with ASP3026 as a single oral dose of 10 mg/kg. After 4 hours, tumors were excised, and total and phosphorylated EML4-ALK were detected by immunoblotting. The numbers represent the mean percentage of phosphorylated protein/total protein relative to that in the vehicle-treated group. ***, $P < 0.001$ compared with the value of the vehicle-treated group (Student *t* test). B, subcutaneously xenografted mice with NCI-H2228 cells were treated with once-daily oral administration of ASP3026 at the indicated doses for two weeks. Crizotinib was given twice daily at the indicated doses. Tumor volume and body weight were measured to assess antitumor activity. Each point represents the mean ± SEM, and the number of animals used is shown in parentheses. The values obtained on day 14 were statistically analyzed and compared. **, $P < 0.01$ compared with the value of the control group on day 14 (Dunnett test). C, ASP3026 concentrations in plasma and tumors after 5-day repeated oral dosing of ASP3026 at the indicated doses in mice with NCI-H2228 tumors were measured using high-performance liquid chromatography-tandem mass spectrometry. Each point represents the mean ± SEM of three individual mice. D, *hEML4-ALK* transgenic mice were treated with once-daily oral administration of ASP3026 at the indicated doses for 11 days. CT acquisition data were reconstructed using Inveon Acquisition Workplace software to determine tumor volume. Each point represents the mean ± SEM ($n = 3$–4). **, $P < 0.01$; ***, $P < 0.001$ compared with the value of the control group by two-way ANOVA followed by Bonferroni multiple comparison test. n.d., not detected.

Fig. S3). Using this model, we also evaluated and compared the efficacy of once-daily oral dosing of ASP3026 and crizotinib. Median survival time (MST) was 39 days in vehicle-treated control mice and 71 days in crizotinib-treated mice at 30 mg/kg (Fig. 4A). In contrast, no mice receiving ASP3026 treatment at 30 mg/kg died during the 90-day experimental period (Fig. 4A). The mortality effects were accompanied by changes in the bioluminescent emissions, with crizotinib-treated mice at 30 mg/kg showing increased emissions after an initial reduction, whereas ASP3026-induced reduction of emissions at 30 mg/kg continued throughout the experimental period (Fig. 4B). The mean bioluminescent emission in the ASP3026-treated group was significantly lower than that in the crizotinib-treated group, indicating that the ASP3026-treated animals exhibited a lower tumor burden.

ASP3026 shows antitumor efficacy against ALK-dependent NSCLC tumors in liver

As the liver is one of the metastatic sites in crizotinib-treated patients with EML4-ALK–positive NSCLC (28),

Published OnlineFirst January 13, 2014; DOI: 10.1158/1535-7163.MCT-13-0395

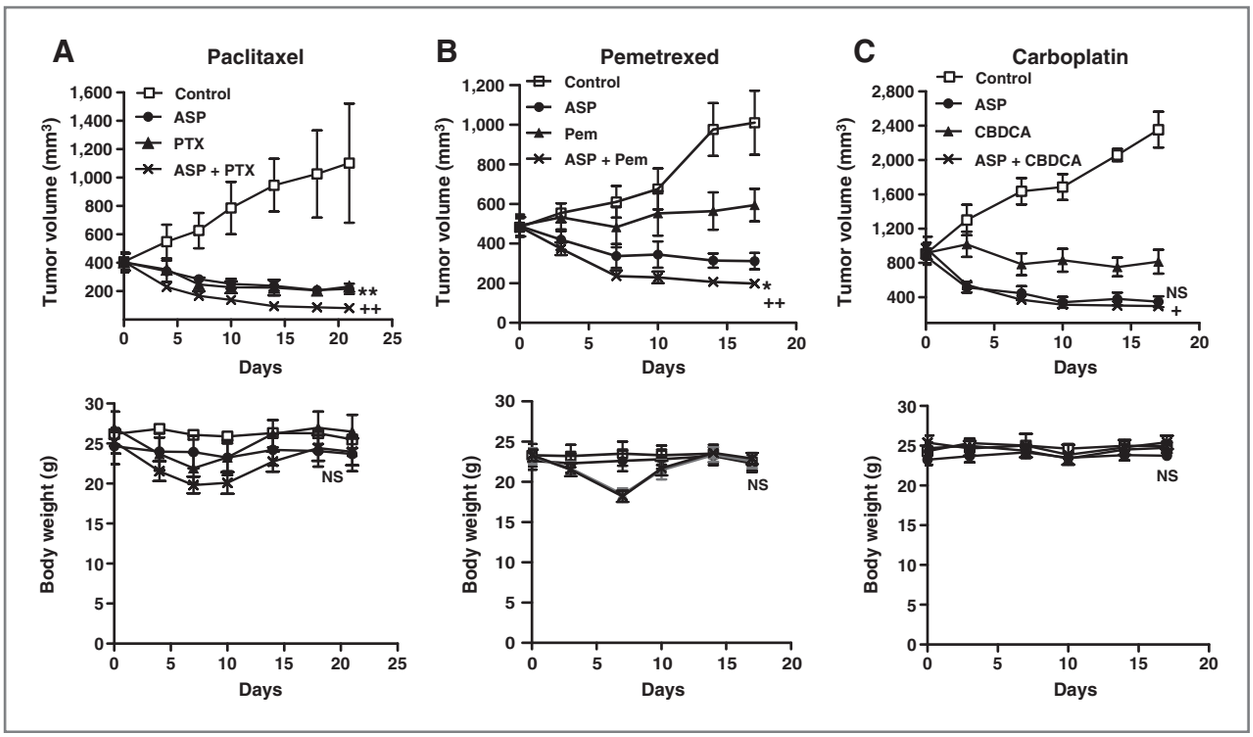

Figure 3. Antitumor activity of ASP3026 in combination with antitumor agents against NCI-H2228 tumors. Oral ASP3026 was given once daily at 10 mg/kg in combination with (A) paclitaxel (intravenous, 12 mg/kg, days 0–4), (B) pemetrexed (intravenous, 50 mg/kg, days 0–4), or (C) carboplatin (intravenous, 60 mg/kg, days 0 and 7). Tumor volume and body weight were measured to assess antitumor activity. Each point represents the mean ± SEM ($n = 4$–5). Values obtained on the last day of each experiment were statistically analyzed and compared. *, $P < 0.05$; **, $P < 0.01$ compared with the ASP3026 single-treatment group, +, $P < 0.05$; ++, $P < 0.01$ compared with each combination partner (Student t test). NS, not significant.

we evaluated the antitumor activity of ASP3026 against tumors in the liver. H2228-luc cells were inoculated into the portal vein of mice, and the implanted cells were monitored using BLI of the upper abdominal area (Fig. 4C). The bioluminescent emissions of inoculated animals decreased during the initial 10 days after inoculation and showed an approximately 100-fold increase during the subsequent 30 days, with tumors forming in entire lobes of the liver (Supplementary Fig. S4). During the first 10 days of the treatment, crizotinib at 30 mg/kg as a once daily oral dose reduced the BLI signal intensity to one third of that at the initiation of treatment (3.2×10^8 to 1.1×10^8 photons/sec), but the emission increased between days 10 and 20 (1.1×10^8 to 2.0×10^8 photons/sec), which is a similar finding to that observed in the intrapleural xenograft model (Fig. 4C). In contrast, the emission was reduced to approximately 1/100 of that at the initiation of treatment by 30 mg/kg ASP3026 as a once daily oral dose for 14 days (3.3×10^8 to 4.2×10^6 photons/sec), and reached 7.7×10^5 photons/sec by the end of the 19-day experimental period (Fig. 4C).

ASP3026 induces regression of tumors harboring gatekeeper-residue mutation L1196M of EML4-ALK

Mutations in the ALK kinase domain that confer resistance to crizotinib were previously identified, following sequence analysis of tumor cells derived from a pleural effusion of a crizotinib-relapsed patient who experienced disease progression after a partial response (31). One of the mutations, L1196M, was observed at a gatekeeper position, and it was confirmed that crizotinib shows less inhibitory activity against mutated EML4-ALK with L1196M. To assess the inhibitory activity of ASP3026 against mutated EML4-ALK, here, *in vitro* kinase inhibitory, *in vitro* antiproliferative, and *in vivo* antitumor assays were conducted. ASP3026 inhibited the kinase activities of wild-type and mutated EML-ALKs with IC_{50} values of 10 and 32 nmol/L, respectively, whereas crizotinib displayed 10-fold weaker activity for mutated EML4-ALK compared with wild-type (Supplementary Table S4A). In the spheroid cell culture system, both compounds concentration-dependently inhibited the growth of 2-day treated cells, and the IC_{50} values showed a similar tendency to the kinase inhibitory activities. The IC_{50} ratios of ASP3026 and crizotinib against L1196M/3T3 cells versus EML4-ALK/3T3 cells were 3.9 and 9.2, respectively (Supplementary Table S4B). In addition, crizotinib at 100 mg/kg as a once daily oral dose for 4 days showed no efficacy against L1196M/3T3 tumors, but did induce the regression of EML4-ALK/3T3 tumors (Fig. 5A and B). In contrast, ASP3026 induced tumor regression at 100 mg/kg in both models (Fig. 5A and B), indicating the

Published OnlineFirst January 13, 2014; DOI: 10.1158/1535-7163.MCT-13-0395

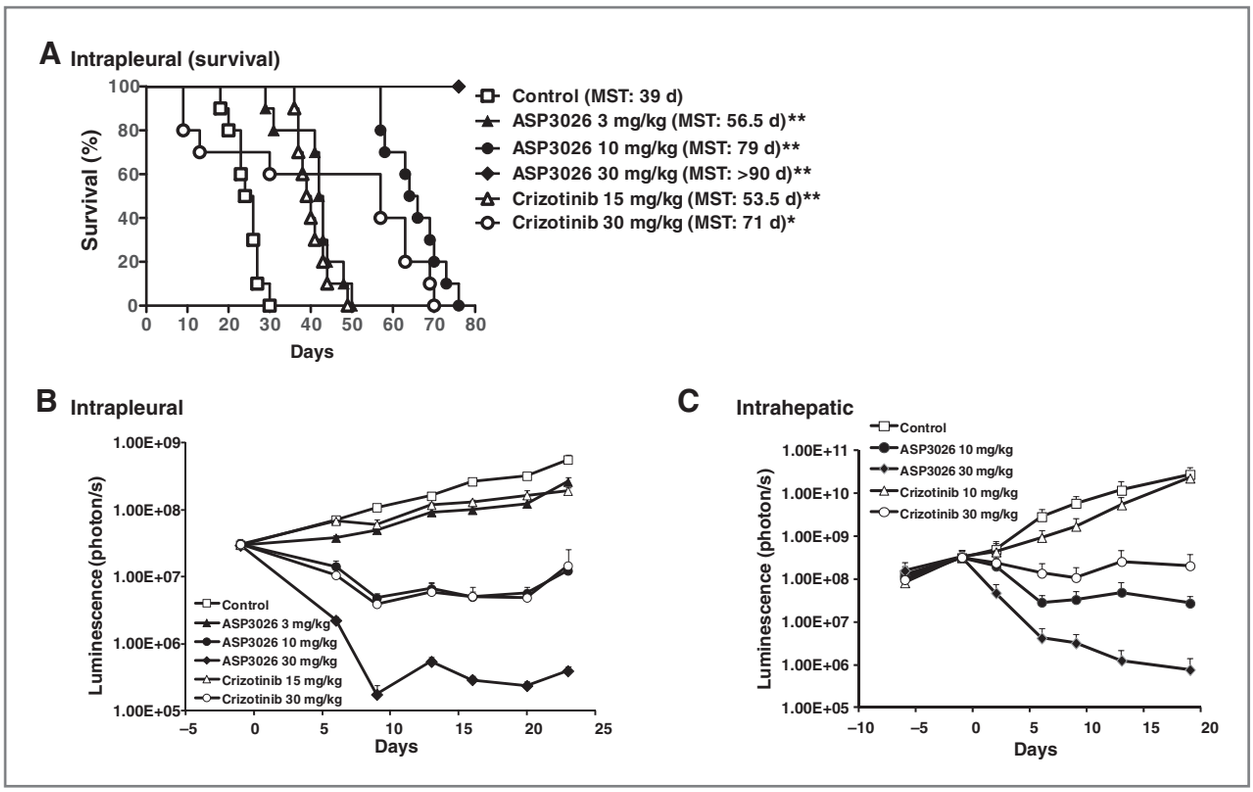

Figure 4. Antitumor activity of ASP3026 against tumors in the pleural cavity and liver. A, H2228-luc cells were directly inoculated into the pleural cavity of NOD/SCID mice. ASP3026 and crizotinib were orally administered once daily for 7 weeks at doses ranging from 3 to 30 mg/kg starting at 14 days after cell inoculation ($n = 10$). The survival of mice was monitored daily, and the MST was determined for each group. *, $P < 0.05$; **, $P < 0.01$ compared with the value of the control group by the log-rank test. B, ASP3026 and crizotinib were administered to NOD/SCID mice implanted with H2228-luc cells as in A, and the implanted cells were monitored using BLI of the chest area. Each point represents the mean BLI ± SEM ($n = 8$). C, H2228-luc cells were inoculated into the portal vein of NOD/SCID mice. After confirming tumor growth, ASP3026 and crizotinib were orally administered once daily for three weeks at the indicated doses. Each point represents the mean BLI ± SEM from each animal ($n = 8$).

therapeutic potential of this drug for patients who are resistant/refractory to crizotinib.

To further understand and compare the inhibitory activity of ASP3026 and crizotinib against mutated EML4-ALK with L1196M, computational modeling of the wild-type and L1196M ALK tyrosine kinase domains was performed (Fig. 5C). The modeling revealed that wild-type ALK had sufficient space for crizotinib to fit within the ATP-binding pocket, whereas the L1196M mutation limits the space available for the methyl group at the benzyl position of crizotinib due to the larger side-chain of methionine compared with leucine. In contrast, ASP3026 was well docked with both wild-type and L1196M ALK.

Discussion

The discovery of EML4-ALK as a drug-targetable cancer driver led to the development of the ALK inhibitor crizotinib, which showed high efficacy in clinical trials with patients with NSCLC harboring this oncogenic kinase, with overall response rates of ≥50% (28, 29). However, the treatment was not curative, and the patients developed resistance to crizotinib in brain, liver, and lung tissues with a progression-free survival of only approximately 10 months (28–30). Therefore, a need exists for the development of novel ALK inhibitors and drug combinations to further improve treatment outcomes.

In the present study, we demonstrated that ASP3026 has growth-inhibitory activity that is accompanied by a decrease of phosphorylated ALK in NCI-H2228 ALK-fusion–positive NSCLC cells. In mice xenografted with NCI-H2228 cells, ASP3026 showed antitumor activity with a wide therapeutic margin between efficacious and toxic doses. ASP3026 induced tumor regression at oral doses of 3 mg/kg or more, with no apparent toxicity or body weight loss, even at a dose of 100 mg/kg. The broad therapeutic margin of ASP3026 is possibly due to its high uptake in tumors, higher ALK selectivity, and different spectrum of kinase inhibition compared with crizotinib. In the *hEML4-ALK* transgenic mouse model, ASP3026 also showed potent antitumor activity, as assessed by tumor shrinkage in the lung to nondetectable levels in CT scans. Notably, however, ASP3026 at 10 mg/kg did not induce tumor regression in this model, possibly due to

Published OnlineFirst January 13, 2014; DOI: 10.1158/1535-7163.MCT-13-0395

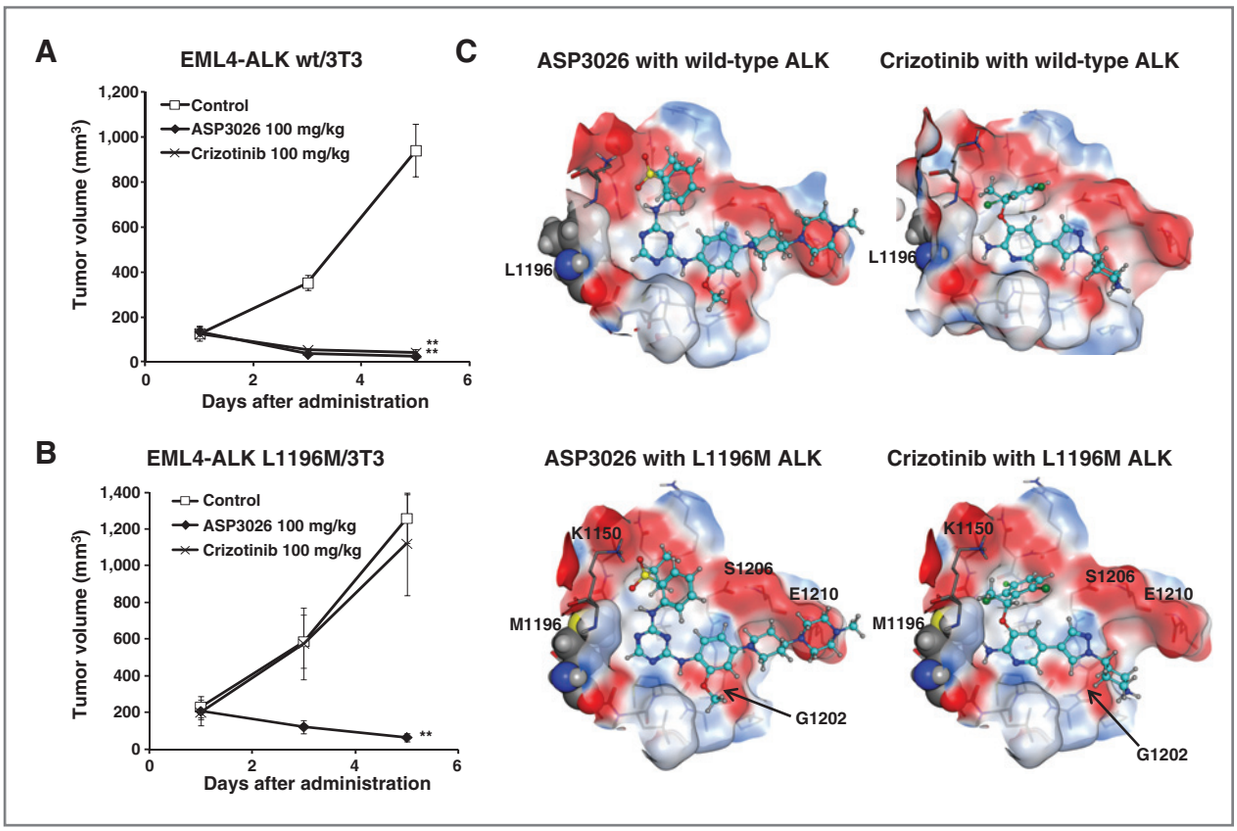

Figure 5. Antitumor activity of ASP3026 against tumor cells expressing a gatekeeper-residue mutant of EML4-ALK, and binding modes of ASP3026 and crizotinib with wild-type and L1196M ALKs. EML4-ALK/3T3 (A) and EML4-ALK L196M/3T3 cells (B) were subcutaneously inoculated into nude mice, and ASP3026 and crizotinib were then administered to mice as a daily oral dose of 100 mg/kg/day for 5 days. Tumor volume was measured to assess antitumor activity. Each data point represents the mean ± SEM ($n = 4$). **, $P < 0.01$ compared with the value of the control group on day 5 (Dunnett test). C, ASP3026 and crizotinib are shown as ball-and-stick models and the gatekeeper residues (L1196 and M1196) are drawn as vdW spheres. Atoms are colored by element: white, hydrogen; cyan, carbon of ligands; gray, carbon of proteins; blue, nitrogen; red, oxygen; and yellow, sulfur. The protein surface is colored on the basis of electrostatic potential (blue, positive; red, negative; and white, neutral). For clarity, nonpolar hydrogen atoms are omitted and the protein surfaces lying anterior to the gatekeeper residues are hidden. G1202, E1210, and S1206 are potential interactive sites with the piperidine ring of crizotinib and the piperazine ring of ASP3026. The K1150 residue forms a hydrogen bond with the sulfonyl group of ASP3026.

differences in the rate of tumor growth and/or ALK dependency between *hEML4-ALK* transgenic mice and NCI-H2228 xenografted mice. This finding was also supported by the higher concentration of orally administered ASP3026 in the lung compared with plasma. In a preliminary study of antiproliferative assays using 145 types of NSCLC-derived cell lines, only five cell lines with ALK fusions, including NCI-H2228 and H3122, were sensitive (>50% inhibition at 300 nmol/L) to ASP3026 (data not shown), indicating that this compound has selective inhibitory activity against ALK-dependent cancer cells. This fact might be reflected in the low toxic profile of ASP3026.

In intrapleural and intrahepatic xenograft models of NOD/SCID mice with NCI-H2228 tumors, crizotinib at 30 mg/kg induced tumor regression during the initial treatment phase, but tumors then increased in size despite continuation of oral dosing of crizotinib. The plasma concentrations of crizotinib were 1.3, 1.5, and 1.3 μg/mL at 2, 4, and 8 hours after 14-day repeated oral administration at 30 mg/kg in mice with intrahepatic xenografts (data not shown). In patients with ALK fusion–positive NSCLC, the median trough concentration of crizotinib at steady state is reported to be approximately 0.3 μg/mL (37). On the basis of the reported clinical data, we consider that sufficient drug exposure was achieved in mice administered 30 mg/kg crizotinib. In the two xenograft models, treatment with 30 mg/kg ASP3026 induced continuous tumor reduction, indicating that ASP3026 has potential efficacy against metastatic lesions in patients refractory to crizotinib, although this conclusion should be reevaluated once pharmacokinetic data in humans become available.

The gatekeeper-residue mutation L1196M of ALK was initially found in patients with ALK-positive NSCLC who relapsed after an initial response to crizotinib (31, 38–40). In our present experiments, crizotinib exhibited 10-fold weaker inhibitory activity against EML4-ALK with

Published OnlineFirst January 13, 2014; DOI: 10.1158/1535-7163.MCT-13-0395

L1196M compared with wild-type EML4-ALK, and no inhibitory activity was detected in a xenograft model at an oral daily dose of 100 mg/kg, as was shown in previous reports (24, 25). The inhibitory activity of ASP3026 was approximately 3-fold weaker for EML4-ALK with the L1196M mutation, but in the xenograft model, ASP3026 also induced tumor regression in cells expressing this gatekeeper-residue mutant as well as wild-type EML4-ALK. In addition, computation modeling suggested that ASP3026 fits more deeply within the ATP-binding pocket of the gatekeeper-residue mutant form of EML4-ALK than crizotinib, which might explain why ASP3026 showed more potent efficacy within the therapeutic margin compared with crizotinib.

ASP3026 induced rapid tumor regression in subcutaneous, intrapleural, and intra-hepatic NCI-H2228 xenograft and transgenic mouse models. In these models, tumors rapidly decreased in size during the first 10 days of treatment with ASP3026, but the tumor regression then slowed. In the xenograft models, tumors were detectable at the end of each treatment period, with the size of the remaining tumors exhibiting a dependence on the dose of ASP3026. When the remaining tumors were again grown and treated with ASP3026 after a washout period of 3 weeks, the tumors rapidly decreased in size (data not shown), indicating that the remaining tumor cells are considered to retain ALK fusion kinases. Although the mechanism underlying the reduced rate of tumor regression is unknown, it is possible that alternative pathways, such as those involving other tyrosine kinases, are upregulated in the residual tumors. In patients refractory to crizotinib, the EGFR pathway is activated because of EGFR upregulation, active mutation of EGFR, and increased ligand concentrations in pleural effusion (38–40). In addition, *KIT* gene amplification and *KRAS* mutation were also found in crizotinib-refractory patients, suggesting that several alternative pathways are possibly involved in the refractory response (38, 39). The findings of several preclinical studies also indicate that alternative pathways may play an important role in resistance to crizotinib. For example, several EGFR ligands, including EGF, TGF-α, and HB-EGF, triggered resistance to ALK inhibitors against ALK-dependent cells (41), and coactivation of EGFR signaling was observed in ALK inhibitor–resistant H3122 cells (42). Tanizaki and colleagues (43) also demonstrated that EGF-mediated activation of HER family signaling is associated with ALK-TKI resistance in lung cancer positive for EML4-ALK. Thus, the combination therapy of ASP3026 with inhibitors targeting alternative pathways, such as EGFR, might lead to complete tumor regression. In our preliminary experiments, NCI-2228 cells resistant to ASP3026 developed after long-term culture in the presence of 500 to 1,000 nmol/L ASP3026. Elucidation of the resistance mechanism may help determine suitable mechanism-based medicines for treating patients resistant to ASP3026.

In the present study, ASP3026 enhanced the antitumor activity of paclitaxel and pemetrexed in a NCI-H2228 subcutaneous xenograft model, but did not synergistically enhance the activity of carboplatin. Although the reason for this latter result is unknown, importantly, ASP3026 did not enhance the toxicity of these NSCLC drugs. Increasing evidence for intratumor genetic heterogeneity is accumulating, both within individual tumor biopsies and between spatially separated biopsies of the same tumor, suggesting that solid cancer is generally heterogeneous (44, 45). As patients with ALK fusion–positive tumors are also likely to have fusion-negative tumors, the combination of ASP3026 with conventional antitumor drugs may provide therapeutic benefits to patients. Notably, however, the combination of a targeted TKI such as ASP3026 with cytostatic anticancer agents has not yet been proven to be generally effective and further examination of patient-derived xenografts is necessary to evaluate the potential benefits of such combination therapy.

In conclusion, ASP3026 selectively inhibits ALK kinases and has high antitumor activity and tumor penetration against ALK-driven tumors, leading to prolonged survival. ASP3026 also has a wide therapeutic margin between efficacious and toxic doses, and exhibits efficacy against crizotinib-refractory tumors. Notably, combining ASP3026 with antitumor agents enhances the activity of these compounds. Our findings demonstrate that ASP3026 functions as a novel ALK inhibitor and is expected to improve the therapeutic outcomes of patients with cancer with ALK abnormality.

Disclosure of Potential Conflicts of Interest

M. Mori, N. Shindou, T. Soga, T. Furutani, and S. Kuromitsu have ownership interest in patents WO2009008371 A1 and US20080090776 A1. I. Shimada and Y. Kondoh have ownership interest in a patent WO2009008371 A1. No potential conflicts of interest were disclosed by the other authors.

Authors' Contributions

Conception and design: M. Mori, Y. Ueno, M. Kudoh, S. Kuromitsu
Development of methodology: Y. Ueno, H. Fushiki, H. Sakagami, T. Furutani
Acquisition of data (provided animals, acquired and managed patients, provided facilities, etc.): M. Mori, Y. Ueno, S. Konagai, H. Fushiki, I. Shimada, N. Shindou, T. Soga, H. Sakagami, T. Furutani, H. Doihara
Analysis and interpretation of data (e.g., statistical analysis, biostatistics, computational analysis): M. Mori, Y. Ueno, S. Konagai, R. Saito, K. Mori
Writing, review, and/or revision of the manuscript: M. Mori, Y. Ueno, S. Konagai, H. Fushiki, Y. Kondoh, R. Saito, K. Mori, H. Sakagami, T. Furutani, S. Kuromitsu
Administrative, technical, or material support (i.e., reporting or organizing data, constructing databases): S. Konagai, Y. Kondoh
Study supervision: M. Kudoh, S. Kuromitsu

Grant Support

This study was sponsored by Astellas Pharma Inc.

The costs of publication of this article were defrayed in part by the payment of page charges. This article must therefore be hereby marked *advertisement* in accordance with 18 U.S.C. Section 1734 solely to indicate this fact.

Received May 16, 2013; revised November 20, 2013; accepted December 13, 2013; published OnlineFirst January 13, 2014.

Published OnlineFirst January 13, 2014; DOI: 10.1158/1535-7163.MCT-13-0395

References

1. Siegel R, Ward E, Brawley O, Jemal A. Cancer statistics, 2011: the impact of eliminating socioeconomic and racial disparities on premature cancer deaths. CA Cancer J Clin 2011;61:212–36.
2. Janku F, Stewart DJ, Kurzrock R. Targeted therapy in non-small-cell lung cancer–is it becoming a reality? Nat Rev Clin Oncol 2010;7: 401–14.
3. Druker BJ, Sawyers CL, Kantarjian H, Resta DJ, Reese SF, Ford JM, et al. Activity of a specific inhibitor of the BCR-ABL tyrosine kinase in the blast crisis of chronic myeloid leukemia and acute lymphoblastic leukemia with the Philadelphia chromosome. N Engl J Med 2001; 344:1038–42.
4. Moen MD, McKeage K, Plosker GL, Siddiqui MA. Imatinib: a review of its use in chronic myeloid leukaemia. Drugs 2007;67:299–320.
5. Baselga J. Clinical trials of single-agent trastuzumab (Herceptin). Semin Oncol 2000;5 Suppl 9:20–6.
6. Paez JG, Jänne PA, Lee JC, Tracy S, Greulich H, Gabriel S, et al. EGFR mutations in lung cancer: correlation with clinical response to gefitinib therapy. Science 2004;304:1497–500.
7. Lynch TJ, Bell DW, Sordella R, Gurubhagavatula S, Okimoto RA, Brannigan BW, et al. Activating mutations in the epidermal growth factor receptor underlying responsiveness of non-small-cell lung cancer to gefitinib. N Engl J Med 2004;350:2129–39.
8. Pao W, Miller V, Zakowski M, Doherty J, Politi K, Sarkaria I, et al. EGF receptor gene mutations are common in lung cancers from "never smokers" and are associated with sensitivity of tumors to gefitinib and erlotinib. Proc Natl Acad Sci U S A 2004;101: 13306–11.
9. Chapman PB, Hauschild A, Robert C, Haanen JB, Ascierto P, Larkin J, et al. Improved survival with vemurafenib in melanoma with BRAF V600E mutation. N Engl J Med 2011;364:2507–16.
10. Soda M, Choi YL, Enomoto M, Takada S, Yamashita Y, Ishikawa S, et al. Identification of the transforming EML4-ALK fusion gene in non-small-cell lung cancer. Nature 2007;448:561–6.
11. Rikova K, Guo A, Zeng Q, Possemato A, Yu J, Haack H, et al. Global survey of phosphotyrosine signaling identifies oncogenic kinases in lung cancer. Cell 2007;131:1190–203.
12. Takeuchi K, Choi YL, Togashi Y, Soda M, Hatano S, Inamura K, et al. KIF5B-ALK, a novel fusion oncokinase identified by an immunohistochemistry-based diagnostic system for ALK-positive lung cancer. Clin Cancer Res 2009;15:3143–9.
13. Soda M, Takada S, Takeuchi K, Choi YL, Enomoto M, Ueno T, et al. A mouse model for EML4-ALK-positive lung cancer. Proc Natl Acad Sci U S A 2008;105:19893–7.
14. Chen Z, Sasaki T, Tan X, Carretero J, Shimamura T, Li D, et al. Inhibition of ALK, PI3K/MEK, and HSP90 in murine lung adenocarcinoma induced by EML4-ALK fusion oncogene. Cancer Res 2010;70: 9827–36.
15. Crystal AS, Shaw AT. New targets in advanced NSCLC: EML4-ALK. Clin Adv Hematol Oncol 2011;9:207–14.
16. Mano H. ALKoma: a cancer subtype with a shared target. Cancer Discov 2012;2:495–502.
17. Ladanyi M. The NPM/ALK gene fusion in the pathogenesis of anaplastic large cell lymphoma. Cancer Surv 1997;30:59–75.
18. Lawrence B, Perez-Atayde A, Hibbard MK, Rubin BP, Dal Cin P, Pinkus JL, et al. TPM3-ALK and TPM4-ALK oncogenes in inflammatory myofibroblastic tumors. Am J Pathol 2000;157:377–84.
19. Debelenko LV, Raimondi SC, Daw N, Shivakumar BR, Huang D, Nelson M, et al. Renal cell carcinoma with novel VCL-ALK fusion: new representative of ALK-associated tumor spectrum. Mod Pathol 2011;24: 430–42.
20. Mariño-Enríquez A, Ou WB, Weldon CB, Fletcher JA, Pérez-Atayde AR. ALK rearrangement in sickle cell trait-associated renal medullary carcinoma. Genes Chromosomes Cancer 2011;50: 146–53.
21. De Paepe P, Baens M, van Krieken H, Verhasselt B, Stul M, Simons A, et al. ALK activation by the CLTC-ALK fusion is a recurrent event in large B-cell lymphoma. Blood 2003;102:2638–41.
22. Janoueix-Lerosey I, Lequin D, Brugières L, Ribeiro A, de Pontual L, Combaret V, et al. Somatic and germline activating mutations of the ALK kinase receptor in neuroblastoma. Nature 2008;455: 967–70.
23. Murugan AK, Xing M. Anaplastic thyroid cancers harbor novel oncogenic mutations of the ALK gene. Cancer Res 2011;71:4403–11.
24. Sakamoto H, Tsukaguchi T, Hiroshima S, Kodama T, Kobayashi T, Fukami TA, et al. CH5424802, a selective ALK inhibitor capable of blocking the resistant gatekeeper mutant. Cancer Cell 2011; 19:679–90.
25. Lovly CM, Heuckmann JM, de Stanchina E, Chen H, Thomas RK, Liang C, et al. Insights into ALK-driven cancers revealed through development of novel ALK tyrosine kinase inhibitors. Cancer Res 2011;71: 4920–31.
26. Kwak EL, Bang YJ, Camidge DR, Shaw AT, Solomon B, Maki RG, et al. Anaplastic lymphoma kinase inhibition in non-small-cell lung cancer. N Engl J Med 2010;363:1693–703.
27. Butrynski JE, D'Adamo DR, Hornick JL, Dal Cin P, Antonescu CR, Jhanwar SC, et al. Crizotinib in ALK-rearranged inflammatory myofibroblastic tumor. N Engl J Med 2010;363:1727–33.
28. Camidge DR, Bang YJ, Kwak EL, Iafrate AJ, Varella-Garcia M, Fox SB, et al. Activity and safety of crizotinib in patients with ALK-positive non-small-cell lung cancer: updated results from a phase 1 study. Lancet Oncol 2012;13:1011–9.
29. Riely GJ, Evans TL, Salgia R, Ou S, Gettinger SN, Otterson GA, et al. Results of a global phase II study with crizotinib in advanced ALK-positive non-small cell lung cancer (NSCLC). J Thorac Oncol 2012;7 Supple 4:abstract 3.
30. Camidge DR, Doebele RC. Treating ALK-positive lung cancer–early successes and future challenges. Nat Rev Clin Oncol 2012;9: 268–77.
31. Choi YL, Soda M, Yamashita Y, Ueno T, Takashima J, Nakajima T, et al. ALK Lung Cancer Study Group. EML4-ALK mutations in lung cancer that confer resistance to ALK inhibitors. N Engl J Med 2010;363: 1734–9.
32. Pao W, Miller VA, Politi KA, Riely GJ, Somwar R, Zakowski MF, et al. Acquired resistance of lung adenocarcinomas to gefitinib or erlotinib is associated with a second mutation in the EGFR kinase domain. PLoS Med 2005;2:e73.
33. Branford S, Rudzki Z, Walsh S, Grigg A, Arthur C, Taylor K, et al. High frequency of point mutations clustered within the adenosine triphosphate-binding region of BCR/ABL in patients with chronic myeloid leukemia or Ph-positive acute lymphoblastic leukemia who develop imatinib (STI571) resistance. Blood 2002;99:3472–5.
34. Lu L, Ghose AK, Quail MR, Albom MS, Durkin JT, Holskin BP, et al. ALK mutants in the kinase domain exhibit altered kinase activity and differential sensitivity to small molecule alk inhibitors. Biochemistry 2009;48:3600–9.
35. Kondoh Y, Iikubo K, Kuromitsu S, Shindo N, Soga T, Furutani T, et al., inventors; Astellas Pharma Inc., assignee. Di(arylamino)aryl compound. WO 2009/008371 A1 2009 Jan 15.
36. Galkin AV, Melnick JS, Kim S, Hood TL, Li N, Li L, et al. Identification of NVP-TAE684, a potent, selective, and efficacious inhibitor of NPM-ALK. Proc Natl Acad Sci USA 2007;104:270–5.
37. Tan W, Wilner KD, Bang Y, Kwak EL, Maki RG, Camidge DR, et al. Pharmacokinetics (PK) of PF-02341066, a dual ALK/MET inhibitor after multiple oral doses to advanced cancer patients. J Clin Oncol 28:15s, 2010 (suppl; abstr 2596).
38. Katayama R, Shaw AT, Khan TM, Mino-Kenudson M, Solomon BJ, Halmos B, et al. Mechanisms of acquired crizotinib resistance in ALK-rearranged lung cancers. Sci Transl Med 2012;4:120–31.
39. Doebele RC, Pilling AB, Aisner DL, Kutateladze TG, Le AT, Weickhardt AJ, et al. Mechanisms of resistance to crizotinib in patients with ALK gene rearranged non-small cell lung cancer. Clin Cancer Res 2012;18:1472–82.
40. Kim S, Kim TM, Kim DW, Go H, Keam B, Lee SH, et al. Heterogeneity of genetic changes associated with acquired crizotinib resistance in ALK-rearranged lung cancer. J Thorac Oncol 2013;8: 415–22.
41. Yamada T, Takeuchi S, Nakade J, Kita K, Nakagawa T, Nanjo S, et al. Paracrine receptor activation by microenvironment triggers bypass

Published OnlineFirst January 13, 2014; DOI: 10.1158/1535-7163.MCT-13-0395

survival signals and ALK inhibitor resistance in EML4-ALK lung cancer cells. Clin Cancer Res 2012;18:3592–602.

42. Sasaki T, Koivunen J, Ogino A, Yanagita M, Nikiforow S, Zheng W, et al. A novel ALK secondary mutation and EGFR signaling cause resistance to ALK kinase inhibitors. Cancer Res 2011;71:6051–60.
43. Tanizaki J, Okamoto I, Okabe T, Sakai K, Tanaka K, Hayashi H, et al. Activation of HER family signaling as a mechanism of acquired resistance to ALK inhibitors in EML4-ALK-positive non-small cell lung cancer. Clin Cancer Res 2012;18:6219–26.
44. Swanton C. Intratumor heterogeneity: evolution through space and time. Cancer Res 2012;72:4875–82.
45. Gerlinger M, Rowan AJ, Horswell S, Larkin J, Endesfelder D, Gronroos E, et al. Intratumor heterogeneity and branched evolution revealed by multiregion sequencing. N Engl J Me 2012;366:883–92.

Published OnlineFirst January 13, 2014; DOI: 10.1158/1535-7163.MCT-13-0395

Molecular Cancer Therapeutics

The Selective Anaplastic Lymphoma Receptor Tyrosine Kinase Inhibitor ASP3026 Induces Tumor Regression and Prolongs Survival in Non–Small Cell Lung Cancer Model Mice

Masamichi Mori, Yoko Ueno, Satoshi Konagai, et al.

Mol Cancer Ther 2014;13:329-340. Published OnlineFirst January 13, 2014.